Critical role for αvβ6 integrin in enamel biomineralization

Leila Mohazab[1], Leeni Koivisto[1], Guoqiao Jiang[1], Leena Kytömäki[2], Markus Haapasalo[1], Gethin R. Owen[1], Colin Wiebe[1], Yanshuang Xie[1], Kristiina Heikinheimo[3], Toshiyuki Yoshida[4], Charles E. Smith[5], Jyrki Heino[6], Lari Häkkinen[1], Marc D. McKee[5] and Hannu Larjava[1],*

[1]Faculty of Dentistry, Department of Oral Biological and Medical Sciences, University of British Columbia, Vancouver, BC, Canada
[2]Finnish Microarray and Sequencing Centre, Turku Centre for Biotechnology, University of Turku and Åbo Akademi University, Turku, Finland
[3]Institute of Dentistry, University of Turku and Turku University Hospital, Turku, Finland
[4]Institute of Biotechnology, University of Helsinki, Helsinki, Finland
[5]Faculty of Dentistry and Department of Anatomy and Cell Biology, McGill University, Montreal, QC, Canada
[6]Department of Biochemistry, Turku Centre for Biotechnology, University of Turku, Turku, Finland

*Author for correspondence (larjava@dentistry.ubc.ca)

Summary

Tooth enamel has the highest degree of biomineralization of all vertebrate hard tissues. During the secretory stage of enamel formation, ameloblasts deposit an extracellular matrix that is in direct contact with the ameloblast plasma membrane. Although it is known that integrins mediate cell–matrix adhesion and regulate cell signaling in most cell types, the receptors that regulate ameloblast adhesion and matrix production are not well characterized. We hypothesized that αvβ6 integrin is expressed in ameloblasts where it regulates biomineralization of enamel. Human and mouse ameloblasts were found to express both β6 integrin mRNA and protein. The maxillary incisors of $Itgb6^{-/-}$ mice lacked yellow pigment and their mandibular incisors appeared chalky and rounded. Molars of $Itgb6^{-/-}$ mice showed signs of reduced mineralization and severe attrition. The mineral-to-protein ratio in the incisors was significantly reduced in $Itgb6^{-/-}$ enamel, mimicking hypomineralized amelogenesis imperfecta. Interestingly, amelogenin-rich extracellular matrix abnormally accumulated between the ameloblast layer of $Itgb6^{-/-}$ mouse incisors and the forming enamel surface, and also between ameloblasts. This accumulation was related to increased synthesis of amelogenin, rather than to reduced removal of the matrix proteins. This was confirmed in cultured ameloblast-like cells, in which αvβ6 integrin was not an endocytosis receptor for amelogenins, although it participated in cell adhesion on this matrix indirectly via endogenously produced matrix proteins. In summary, integrin αvβ6 is expressed by ameloblasts and it plays a crucial role in regulating amelogenin deposition and/or turnover and subsequent enamel biomineralization.

Key words: Integrin, Amelogenin, Enamel, Mineralization, Attrition

Introduction

Enamel is the hardest mineralized tissue in the body and the only calcified tissue that is produced by epithelium-derived cells, namely ameloblasts. Amelogenesis consists of secretory, transition and maturation stages (Simmer et al., 2010). During the secretory stage, ameloblasts secrete enamel proteins such as amelogenin (the most abundant enamel matrix protein; Eastoe, 1979), ameloblastin (Krebsbach et al., 1996) and enamelin (Hu et al., 1997) into the enamel matrix. This extracellular matrix undergoes enzymatic modification by enamelysin (MMP-20) and kallikrein 4 (KLK4) in the transition and maturation stages, which results in the formation of a mature enamel that is mainly composed of hydroxyapatite crystallites and a minor amount of residual proteins (Bartlett et al., 1996; Nanci and Smith, 2000). Mutations in amelogenin, enamelin, MMP-20 and KLK4 genes all cause human hereditary amelogenesis imperfecta (AI), in which both enamel formation and its mineralization are affected (Hu et al., 2007). This leads to extensive wear and decay in both the primary and permanent dentition, which may result in tooth loss at a young age or require extensive restorative procedures (Crawford et al., 2007).

During amelogenesis, the apical ameloblast plasma membrane directly abuts against the matrix and the developing enamel crystals (Nanci and Smith, 2000). Although integrins mediate cell-matrix adhesion and signaling in most cell types (Hynes, 2004), the receptors of ameloblasts that mediate ameloblast–matrix adhesion, matrix organization, and signaling are not well characterized. The rat incisor enamel organ has been reported to express the β6 integrin transcript, but its role in enamel formation is not known (Moffatt et al., 2006). Integrin αvβ6 is an epithelial cell-specific integrin that binds to the arginine-glycine-aspartic acid (RGD) amino acid motif in its ligands (Breuss et al., 1993), which include fibronectin, tenascin-C, vitronectin and the latency-associated peptide (LAP) of transforming growth factor-β1 (TGF-β1) and TGF-β3. Its binding to the LAP activates the cytokine (Munger et al., 1999). This integrin-mediated activation plays an important anti-inflammatory role in vivo (Yang et al., 2007), as it regulates experimental TGF-β1-dependent fibrosis in various organs (Hahm et al., 2007; Horan et al., 2008; Patsenker et al., 2008). Furthermore, αvβ6 integrin is expressed in junctional epithelial cells that mediate gingival soft

tissue adhesion to tooth enamel (Ghannad et al., 2008). Interestingly, loss of β6 integrin in mice is associated with characteristics of human periodontal disease, suggesting that αvβ6 integrin plays a role in protecting periodontal tissues from inflammatory changes leading to periodontal disease (Ghannad et al., 2008). Junctional epithelium is derived from cells arising from the reduced enamel epithelium during tooth eruption (Schroeder and Listgarten, 1977). In the present study, therefore, we hypothesized that αvβ6 integrin is also expressed in ameloblasts and that lack of its expression is associated with enamel defects. We show that mice deficient in αvβ6 integrin (*Itgb6*$^{-/-}$) have hypomineralized enamel and show excessive accumulation of amelogenin in the mineralizing enamel matrix.

Results

The teeth of *Itgb6*$^{-/-}$ mice have severe attrition and an abnormal enamel surface

Compared to wild-type (WT) mice, *Itgb6*$^{-/-}$ mice had no obvious differences in tooth development or eruption, and there was no malocclusion. However, when incisors of *Itgb6*$^{-/-}$ mice were examined more closely, it became obvious that they differed from those of WT mice. The maxillary incisors of WT mice had a smooth and yellowish surface, whereas *Itgb6*$^{-/-}$ mouse maxillary incisors lacked the yellow pigmentation and were abnormally white. In addition, mandibular incisors of *Itgb6*$^{-/-}$ mice appeared chalky and the tips were noticeably more rounded than those of their WT counterparts (Fig. 1A,B).
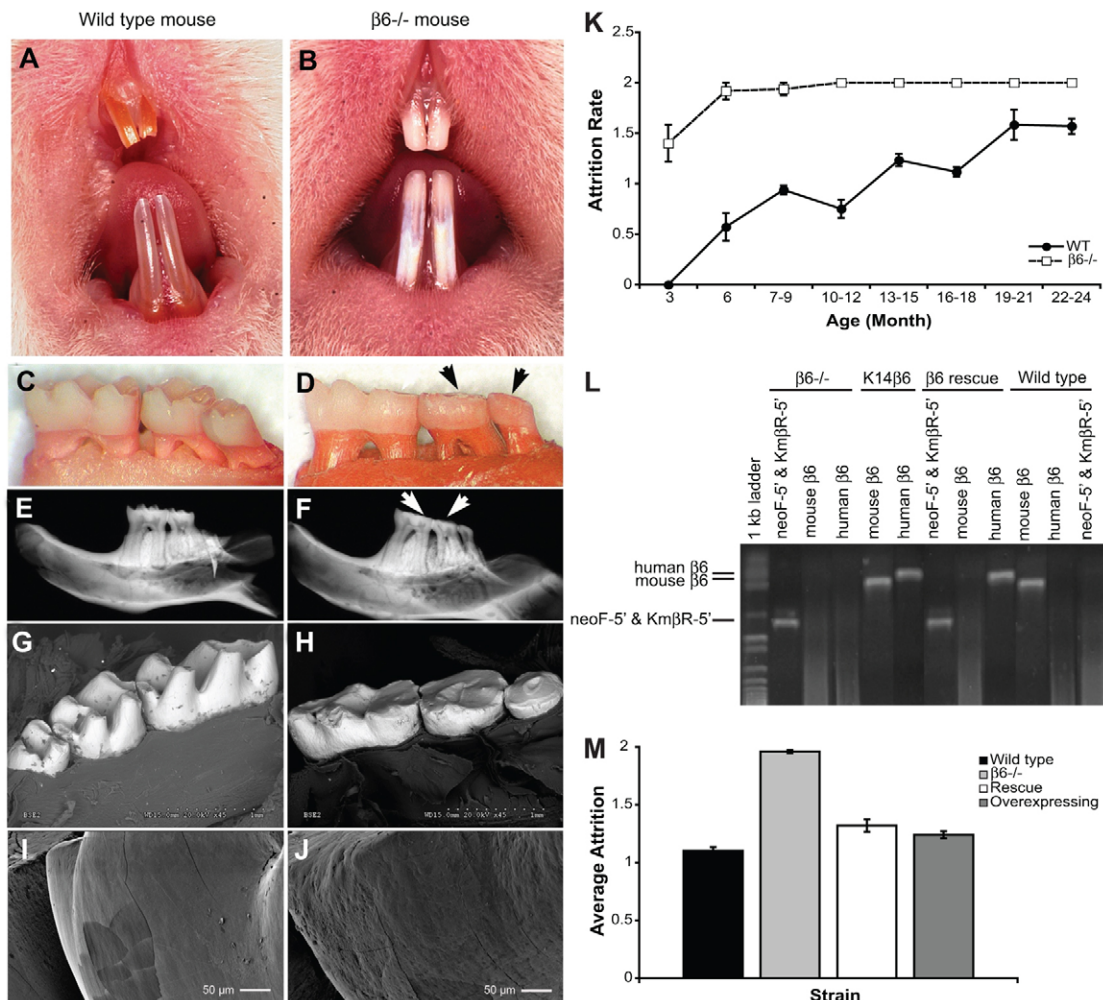
Fig. 1. **Teeth from 6-month-old *Itgb6*$^{-/-}$ mice show severe attrition.** (**A,B**) Incisors of the *Itgb6*$^{-/-}$ (β6−/−) mice show considerable wear at their tips, a chalky appearance and an absence of yellow pigmentation as compared to WT incisors. (**C,D**) Severe attrition is also observed in the *Itgb6*$^{-/-}$ mandibular molars. (**E–H**) High-definition radiographs and backscattered electron SEM images of defleshed mandibles demonstrate occlusal wear to the level of dentin in the *Itgb6*$^{-/-}$ molars. (**I,J**) In secondary electron SEM images, lateral enamel surfaces in *Itgb6*$^{-/-}$ mouse molars appear rough and pitted as compared to those in WT mice. (**K**) In WT mice, the attrition rate increases with age reaching a score (see Materials and Methods) of one in about 12 months. However, attrition in *Itgb6*$^{-/-}$ mice reaches the maximum score of two in 6 months. (**L**) PCR genotyping shows that WT mice express the murine β6 integrin whereas there is no expression in *Itgb6*$^{-/-}$ animals. K14β6 mice have both human and murine β6 integrin. Integrin β6-deficient mice were cross-bred with K14β6 mice to create a β6 integrin rescue line (β6 rescue) carrying only the human β6 integrin gene. The knockout construct was identified with primers for neoF-5′ and KmβR-5′. (**M**) Significant clinical attrition observed in the *Itgb6*$^{-/-}$ mice compared to WT mice can be rescued by human β6 integrin. WT, $n=167$; *Itgb6*$^{-/-}$, $n=124$; rescue, $n=60$; overexpressing, $n=99$.

Examination of defleshed mandibles from 12-month-old mice using a dissecting microscope or after taking high-resolution radiographs showed that whereas WT mouse molars had prominent and pointed cusps on all three molars (Fig. 1C,E,G), the molar cusps of the $Itgb6^{-/-}$ mice had extensive wear at their occlusal surfaces (Fig. 1D,F,H) similar to their blunted incisors. This severe attrition of molar cusps was highly evident in the scanning electron micrographs, displaying flattened and heavily worn $Itgb6^{-/-}$ mouse molar cusps (Fig. 1H). While the WT enamel was smooth, the enamel of $Itgb6^{-/-}$ mice showed extensive pit formation and roughness (Fig. 1I,J). The rate and amount of attrition in the molar teeth was further investigated in different age groups. As expected, as the mice aged the attrition rate increased in both the WT and $Itgb6^{-/-}$ mice; however, the rate of attrition was much faster in the $Itgb6^{-/-}$ group (Fig. 1K). The degree of attrition in the $Itgb6^{-/-}$ mice reached the maximum level already by 6 months when the cusps were almost completely worn down (Fig. 1K).

Next, we investigated whether the enamel phenotype in the $Itgb6^{-/-}$ mice could be rescued by re-expressing β6 integrin. For this purpose, the $Itgb6^{-/-}$ mice were bred with mice overexpressing human β6 integrin under the cytokeratin 14 (K14) promoter in addition to their own endogenous mouse β6 integrin (Häkkinen et al., 2004). Offspring carrying only human β6 integrin on the knockout background were selected to represent the β6 integrin rescue mice (Fig. 1L; integrin expression in the ameloblast layer is presented in Fig. 6A). The incisors of the 'overexpressing' and the 'rescue' mice appeared macroscopically normal (data not shown). The average attrition rate of 6-month-old $Itgb6^{-/-}$ mice was significantly higher when compared to the 'rescue' and 'overexpressing' mice of the same age, indicating that the enamel attrition is effectively rescued by human β6 integrin gene in the $Itgb6^{-/-}$ mice (Fig. 1M). Moreover, overexpression of β6 integrin did not seem to affect enamel formation.

Enamel prism structure and mineralization are severely affected in $Itgb6^{-/-}$ mice

To determine the specific nature of the enamel defects in $Itgb6^{-/-}$ mice, we first observed enamel microstructure. Electron micrographs of surface acid-etched incisors demonstrated a significant difference in prism structure and organization between the WT and $Itgb6^{-/-}$ enamel (Fig. 2A,B). In WT mouse incisors, a parallel and well-organized enamel prism structure in alternating rows was present (Fig. 2A). Interestingly, in the $Itgb6^{-/-}$ incisors, the enamel prism organization was completely lost; the enamel was somewhat layered but showed no regular repeating pattern of prism structure (Fig. 2B).

Next, we compared enamel mineral density in WT and $Itgb6^{-/-}$ mice. Micro-CT images were taken from 14-day-old $Itgb6^{-/-}$ and WT mouse mandibular molars. While the mutant mice teeth appeared generally anatomically normal, the X-ray density of the enamel was greatly reduced in both the first and second molars of the $Itgb6^{-/-}$ mice compared to the WT (Fig. 2C,D). To quantify the difference in mineralization during various stages of enamel formation, we measured the mineral-to-protein ratio of the maxillary and mandibular incisors in both mouse lines by an ashing method. Near the apical loop of the incisors, corresponding to the secretory stage, the mineral-to-protein ratio was similar in WT and $Itgb6^{-/-}$ mice (Fig. 2E,F). However, as the distance from the apical loop increased

(maturation stage starts about 3 mm from the apex), the mineral-to-protein ratio of $Itgb6^{-/-}$ mouse incisors became drastically decreased compared to that of the WT mice. In fact, from the regions that corresponded to the maturation stage and onwards, the WT incisors were so highly mineralized that it was not possible to cut away incisor enamel strips for sampling, whereas the $Itgb6^{-/-}$ incisor enamel strips were easily removed along the entire length of the incisors (strip 9 on maxilla and strip 11 on the mandible). In additional mineral analyses using energy-dispersive X-ray spectroscopy, we studied a number of molar teeth. There was no statistical difference in Ca/P ratios between $Itgb6^{-/-}$ and WT molars with the ratios obtained being typical for hydroxyapatite (data not shown).

Integrin β6 mRNA and protein are expressed by ameloblasts in mouse and human teeth

To demonstrate that the β6 integrin mRNA and protein are expressed in mouse teeth, *in situ* hybridization and immunohistochemical studies were performed. *In situ* hybridization of β6 integrin mRNA with the anti-sense and sense probes was performed in the secretory stage of an upper incisor from a 10-day-old WT mouse. The anti-sense probe demonstrated a strong specific signal that was localized only to the cytoplasm of ameloblasts (Fig. 3A), whereas no signal was detected with the control sense probe (Fig. 3B).

Next, we performed immunostaining of β6 integrin protein in frozen sections from the secretory stage of an upper incisor as well as from developing upper molar cusps from 3-day-old WT mice. In both the incisor and molar teeth, prominent β6 integrin immunoreactivity was localized to the ameloblast layer (Fig. 3C,D). Hematoxylin- and Eosin-stained sections confirmed that the β6 integrin immunoreactivity was indeed localized to the ameloblast cell layer (Fig. 3E,F).

In order to investigate whether expression of β6 integrin in ameloblasts is similar in humans, we immunostained maturation-stage ameloblasts from surgically removed, unerupted human wisdom teeth. Ameloblasts were identified in decalcified sections by morphology as well as by a positive signal for K14 and amelogenin (Fig. 3G–I). The ameloblast layer was strongly labeled with the β6 integrin antibody (Fig. 3J), indicating that expression of αvβ6 integrin is conserved in human ameloblasts.

Expression of amelogenin and enamelin is significantly increased in the $Itgb6^{-/-}$ ameloblast layer

In order to identify the gene expression profile associated with the disturbed mineralization of $Itgb6^{-/-}$ enamel, we removed incisor enamel organs of adult $Itgb6^{-/-}$ and WT mice. A heat map of the differentially expressed genes was generated (Fig. 4A). These data demonstrated significant differences in gene expression profiles in enamel organs between the WT and $Itgb6^{-/-}$ mice. Using the GOrilla Gene Ontology analysis tool, two of the biological processes that show significant differences were identified as 'regulation of biomineralization' and 'osteoblast differentiation' (Fig. 4B). The microarray gene expression results for 'cellular components' and 'biological processes' were further analyzed using DAVID (Database for Annotation, Visualization and Integrated Discovery). In both categories, those genes with significant differences in their expression, including genes relevant to biomineralization, were graphed in a pie chart (Fig. 4C,D, respectively). The rest of the genes were grouped in the 'other' category. For the 'cellular
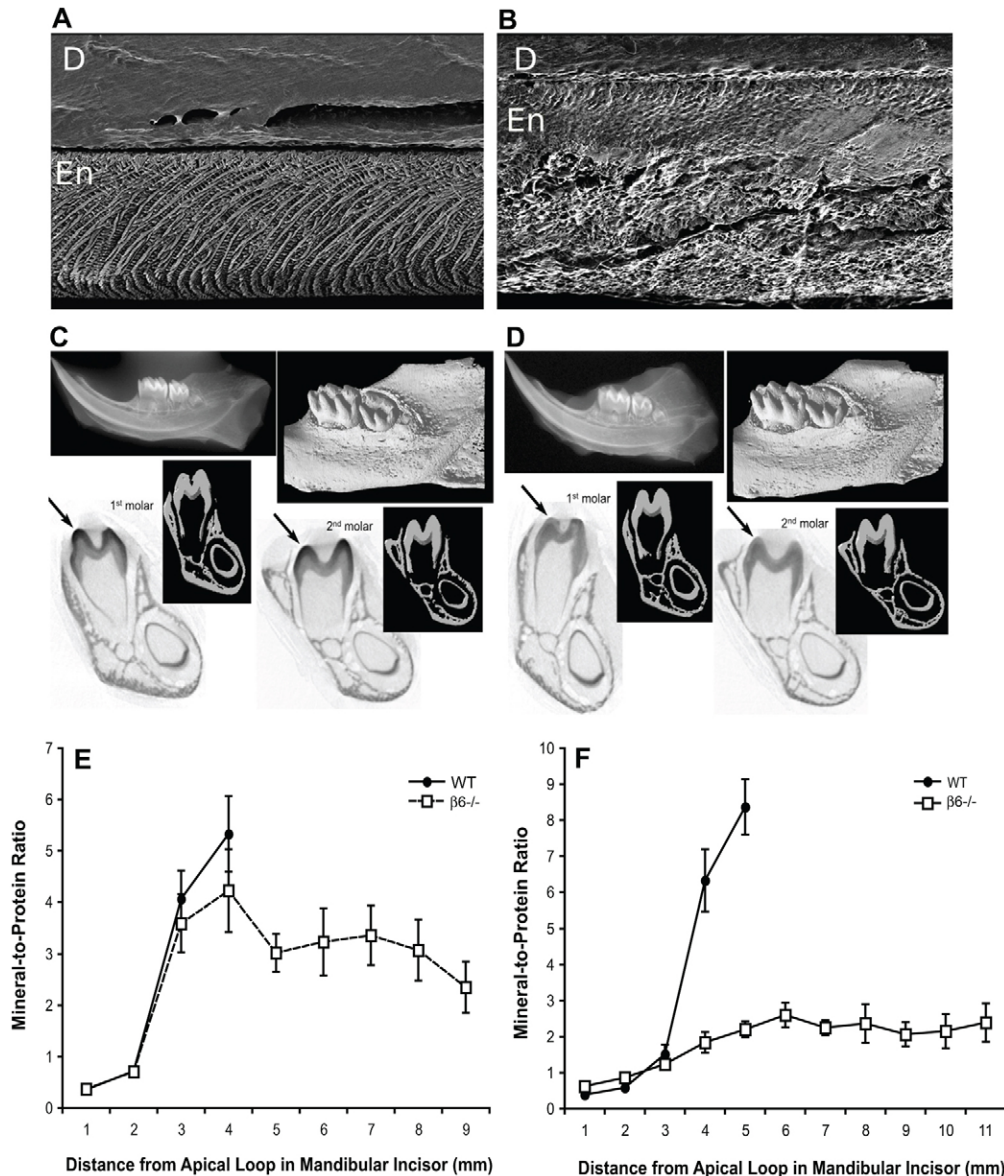
Fig. 2. Enamel prism structure and mineralization are affected in Itgb6$^{-/-}$ mice. (**A**) Enamel in WT mice shows a well-organized and regular prism structure. (**B**) In Itgb6$^{-/-}$ (β6−/−) enamel, the prism structure is completely lost and irregular. D, dentin; En, enamel. (**C,D**) Micro-CT images of mandibular specimens from 14-day-old WT (C) and Itgb6$^{-/-}$ (D) mice show that the general development, relationship with alveolar bone, and eruption of both molars and the incisor appear normal in Itgb6$^{-/-}$ mice. In longitudinal sections of both the first and second molars, the mineral density of enamel appears greatly reduced (less black/dark grey) in Itgb6$^{-/-}$ mice (arrows). (**E,F**) Mineral-to-protein ratios in the maxillary (E) and mandibular (F) incisors of 7-week-old WT and Itgb6$^{-/-}$ mice (n=10) derived from 1-mm strips of developing enamel cut from the apical loop of the incisors and processed for protein and mineral measurements. Strips 1 and 2 represent secretory stage enamel, strips 3 and 4 maturation stage enamel and strips 5–11 mature hard enamel.

component' category, differentially regulated genes included genes associated with extracellular matrix or cell surface. For the 'biological process' category, gene expression for defense, immune response, wounding, cell-cell signaling, endocytosis, tissue morphogenesis and biomineralization differed significantly between the WT and Itgb6$^{-/-}$ mice enamel organs.

The gene profiling analysis showed that 67 genes were downregulated and 171 genes upregulated in Itgb6$^{-/-}$ enamel organs compared to WT enamel organs (absolute fold change >1.6; data not shown). Interestingly, the two most upregulated genes in Itgb6$^{-/-}$ enamel organs were amelogenin (Amelx; 21-fold) and enamelin (Enam; 7.6-fold; Fig. 5A). Other highly upregulated genes were progressive ankylosis gene (Ank; 5-fold) and RNA motif binding proteins (RBMs; data not shown). Expression of Klk4 was also increased, whereas ameloblastin (Ambn), MMP-20 (Mmp20) and amelotin (Amtn) remained unchanged (Fig. 5A, and data not shown). The expression of β1 and β4 integrin genes was not changed, suggesting that there was no compensatory change in other integrins in the absence of

β6 integrin (Fig. 5A). Also, the level of ameloblast marker gene K14 was unchanged. Among the genes that showed the strongest downregulation in the Itgb6$^{-/-}$ enamel organ, were arrestin domain containing 3 protein (Arrdc3; −8-fold), photocadherin-21 (Pcdh21; −5.9-fold) and Fam20B (family with sequence homology 20, member B; −2.9-fold; data not shown). Regulation of these genes in the Itgb6$^{-/-}$ enamel organ may contribute to the hypomineralized enamel phenotype in these animals but their role needs to be further investigated.

Next, we verified the expression levels of amelogenin, enamelin and other key molecules associated with enamel mineralization using quantitative RT-PCR (Fig. 5B). Among the tested mRNAs, only the expression of Amelx, Enam and Klk4 showed significant increases both in gene arrays and in RT-PCR (Fig. 5A,B).

We then verified the integrin expression profiles of the incisor enamel organs of 3–6-month-old WT, Itgb6$^{-/-}$ and β6 integrin rescue mice by western blotting. As expected, Itgb6$^{-/-}$ incisors were negative for β6 integrin, whereas it was expressed in the
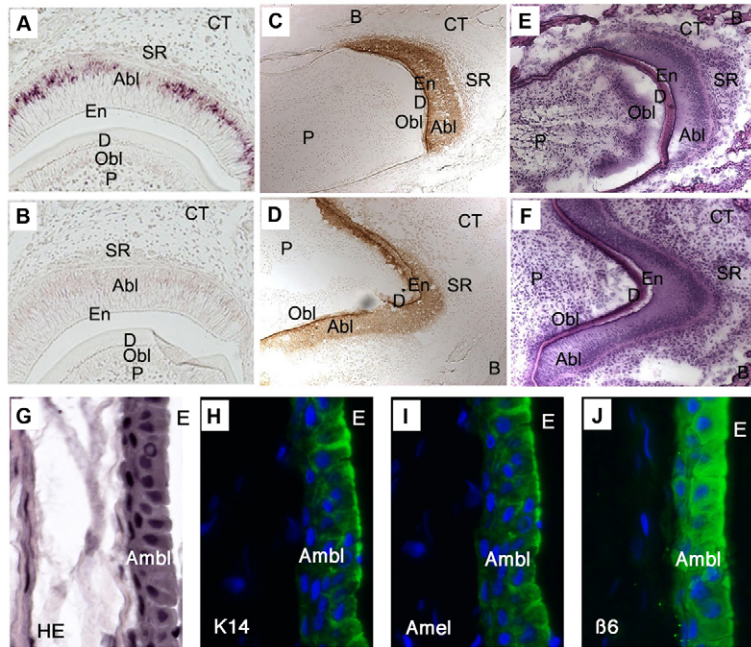
Fig. 3. Integrin β6 mRNA and protein are expressed by ameloblasts in developing mouse and human teeth. (**A,B**) *In situ* hybridization of β6 integrin with anti-sense (A) and sense (B) probes in the secretory stage of a maxillary incisor from a 10-day-old WT mouse. (**C,D**) Immunostaining of β6 integrin protein in undecalcified frozen sections from the secretory stage maxillary incisor (C) and a developing maxillary molar cusp (D) from a 3-day-old WT mouse. (**E,F**) Parallel sections to C and D, respectively, stained with Hematoxylin and Eosin (HE). (**G–I**) Ameloblasts are present on extracted developing human third molars (G; HE staining), and they show positive staining for K14 (H), amelogenin (I) and β6 integrin (J) by immunohistochemistry. Abl/Ambl, ameloblast layer; B, bone; CT, connective tissue; D, forming dentin; En, forming enamel; Obl, odontoblast layer; P, pulp tissue; SR, stellate reticulum.

WT animals (Fig. 6A). In 'rescue' and 'overexpressing' mice, β6 integrin expression was elevated due to the constitutive K14 promoter activity in the enamel organs. Confirming the qRT-PCR results, the expression of β1 integrin was similar in all mouse lines. However, the amount of αv integrin protein, which partners with β6 integrin and others, was reduced in the $Itgb6^{-/-}$ enamel (−2.5-fold; Fig. 6A) likely because of intracellular degradation due to lack of receptor dimerization.

Accumulation of amelogenin protein in the ameloblast layer and enamel of $Itgb6^{-/-}$ mice

Analysis of protein expression in incisor enamel organs of 3- to 6-month-old WT and $Itgb6^{-/-}$ mice by western blotting revealed strong abnormal accumulation of amelogenin in the incisors of $Itgb6^{-/-}$ mice (on average 10-fold; Fig. 6A,C). The main amelogenin bands were between 20 and 25 kDa, which is consistent with major cleaved amelogenins. Consistent with the molar attrition data, the amelogenin accumulation in the incisors of the $Itgb6^{-/-}$ mice was rescued by human β6 integrin expression (Fig. 6A), showing that the accumulation of amelogenin was specifically attributable to β6 integrin deficiency. The expression of MMP-20 and KLK4 was also slightly increased in the $Itgb6^{-/-}$ mice (Fig. 6D). The protein levels of enamelin were not tested because of the lack of availability of a specific antibody for mouse enamelin.

Because one of the main functions of αvβ6 integrin is to activate TGF-β1, we compared the phosphorylation and expression levels of Smad3 and Smad2, downstream targets of TGF-β1, in enamel organs. While TGF-β1 effectively induced pSmad3 phosphorylation in cultured ameloblast-like cells (not shown), there was no significant difference in the expression or phosphorylation of Smad3 or Smad2 between the WT and $Itgb6^{-/-}$ enamel organs (Fig. 6B), suggesting that the mineralization defect and accumulation of amelogenin in the $Itgb6^{-/-}$ enamel is not attributable to impaired TGF-β1 signaling.

To visualize the organization of the ameloblast layer, undecalcified histological sections from the late secretory stage and early maturation stage incisors of 14-day-old $Itgb6^{-/-}$ and WT mice were compared. In WT mice, the ameloblast layer was well organized against mineralizing enamel (Fig. 7A,C). In the $Itgb6^{-/-}$ mice, the ameloblast layer was similarly organized but showed abnormal accumulation of amorphous unmineralized matrix between the cells as well as between the ameloblasts and the forming enamel surface (Fig. 7B,D). In order to identify this material, we performed transmission electron microscopy (TEM) and immunogold labeling for amelogenin localization. Ameloblasts in the WT mouse showed typical organization and secretion of enamel matrix (Fig. 7E) that subsequently became highly mineralized in the maturation stage (Fig. 7I). In the $Itgb6^{-/-}$ ameloblast layer, amorphous protein pools appeared in cyst-like structures between ameloblasts and towards the enamel surface (Fig. 7F,G). By immunolabeling, this material was shown to contain abundant amelogenin (Fig. 7H). Abnormal accumulation of amelogenin was observed both between the cells and within the cells. Electron micrographs of the surface of WT mouse molar enamel revealed a smooth, well organized, and parallel crystal structure at the enamel-ameloblast border (Fig. 7I) in the early maturation stage, whereas corresponding regions in the $Itgb6^{-/-}$ mouse showed an enamel surface that was irregular and layered (Fig. 7J).

Integrin αvβ6 participates indirectly in the adhesion of ameloblast-like cells on amelogenin-rich matrix but not in amelogenin endocytosis

To determine whether ameloblasts use αvβ6 integrin as a cell adhesion receptor for the enamel matrix, we seeded WT mouse ameloblasts in wells coated with a porcine enamel matrix extract (EMD; over 90% amelogenin). Ameloblasts spread on EMD only in the absence of the protein synthesis blocker cycloheximide (Fig. 8A), suggesting that their adhesion on EMD was dependent
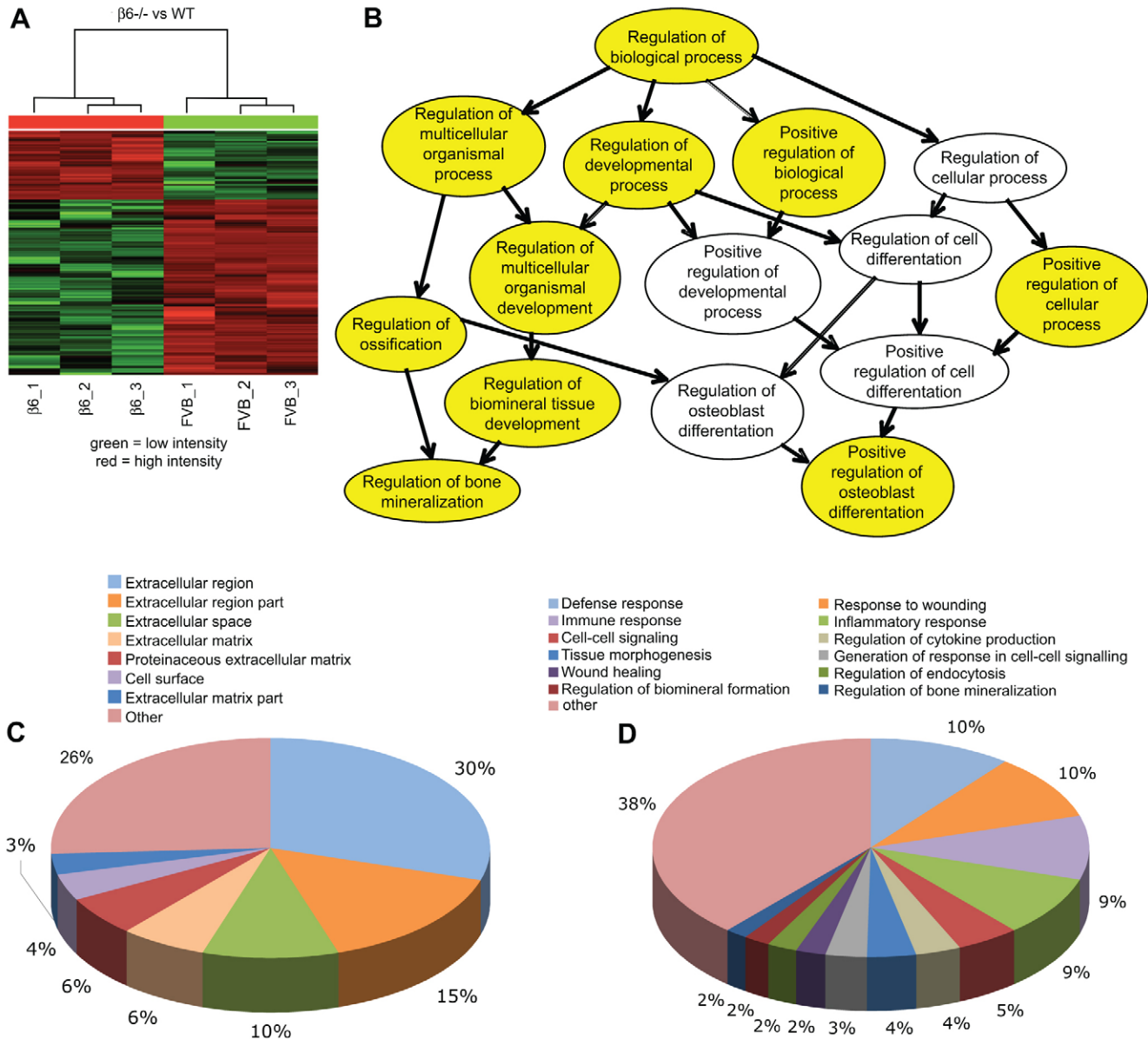
Fig. 4. Gene expression profiling of enamel organs from 6-month-old WT and *Itgb6*$^{-/-}$ mice. (**A**) Heat map of the differentially expressed genes from pooled enamel organs (the groups consisted of four to six mice each and were designated as FVB_1-3 for WT and β6_1-3 for the *Itgb6*$^{-/-}$ mice). (**B**) Differentially regulated biological processes in enamel organs between WT and *Itgb6*$^{-/-}$ mice analyzed using the GOrilla gene ontology analysis tool ($P>10^{-3}$ for the white circles and $P=10^{-3}$–10^{-5} for the yellow circles). (**C,D**) Differentially regulated cellular components (C) and processes (D) between WT and *Itgb6*$^{-/-}$ mice analyzed by the DAVID system.

on endogenous protein synthesis. Stimulating the cells with 200 nM 12-*O*-tetradecanoylphorbol-13-acetate (TPA), an integrin activator, further increased their adhesion and spreading by about 50% (Fig. 8A). To determine whether this adhesion was mediated by αvβ6 integrin, cell spreading was analyzed in the presence of function-blocking anti-αvβ6 integrin antibodies. Three different antibodies blocked 35–50% of the cell spreading in a statistically significant manner (Fig. 8B), indicating that ameloblasts deposit endogenous, amelogenin-binding extracellular matrix proteins, some of which are αvβ6 integrin ligands. As expected, these antibodies did not affect the spreading of *Itgb6*$^{-/-}$ ameloblasts (data not shown).

We next tested whether αvβ6 integrin is involved in the regulation of amelogenin endocytosis in mouse ameloblasts. Amelogenin endocytosis occurred in a similar fashion in both WT and *Itgb6*$^{-/-}$ ameloblasts (Fig. 8C–H), suggesting that αvβ6 integrin does not play a significant role in this internalization process.

Discussion

Epithelial cell integrins regulate a variety of cell functions during development and tissue repair (Larjava et al., 2011). However, little information is available regarding integrin function in ameloblasts during enamel formation. In the present report, we
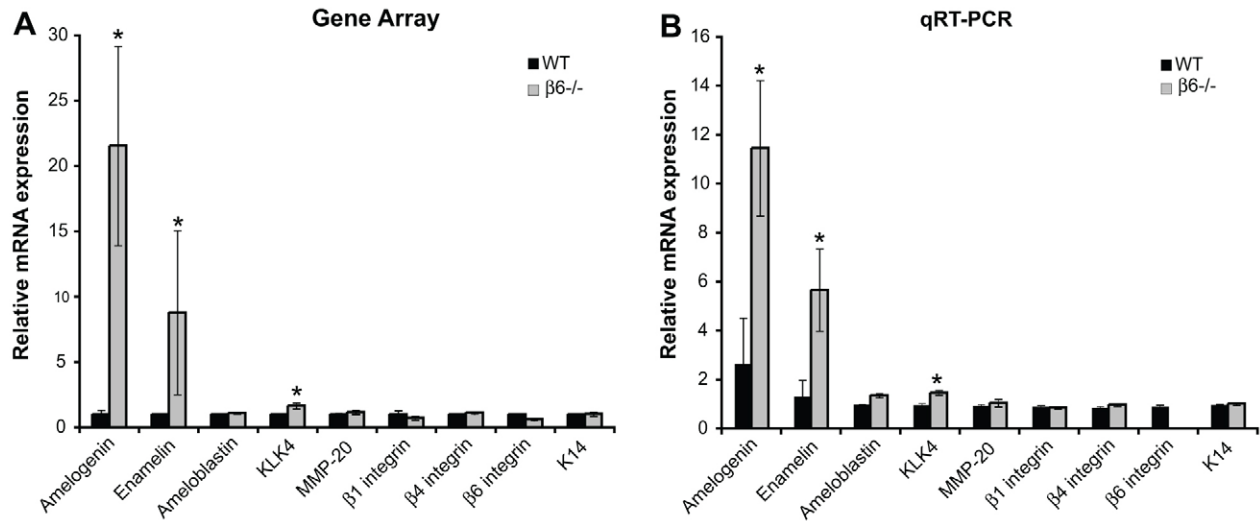
Fig. 5. Relative expression of selected enamel genes in 6-month-old WT and *Itgb6*⁻/⁻ mice. (**A**) Gene profiling; (**B**) confirmation with real-time RT-PCR. Expression of amelogenin, enamelin and KLK4 genes are significantly upregulated in *Itgb6*⁻/⁻ (β6−/−) enamel organs compared to WT enamel organs. Expression of ameloblastin, MMP-20, β1 or β4 integrin and ameloblast marker K14 genes are not significantly altered. Truncated β6 integrin mRNA expressed in the *Itgb6*⁻/⁻ organs was recognized by the gene array probes (A) but was not amplified by the PCR primers specifically designated to detect the translated mRNA (B). *$P<0.05$.

show that αvβ6 integrin plays a crucial role in enamel biomineralization via regulation of amelogenin and enamelin gene expression.

Integrins likely play key roles in tooth development since several integrins, including α6, αv, β1, β4 and β5 integrin subunits, are expressed in the dental epithelium (Salmivirta et al., 1996). Integrin αvβ5 may regulate tooth morphogenesis, as its expression oscillates between dental mesenchyme and epithelium (Yamada et al., 1994). Ameloblasts express α2β1 integrin when they assume their columnar shape (Wu and Santoro, 1994), but no tooth phenotype was observed in α2 integrin knockout mice (unpublished data from our laboratory). Loss-of-function mutations in either α6 or β4 integrin cause human junctional epidermolysis bullosa, in which the epithelium detaches from the basement membrane causing skin or mucosal blistering (Wright, 2010). In these patients, ameloblast adhesion to developing enamel is also reduced, leading to hypoplastic enamel (Wright, 2010).

Only a few potential integrin-binding ligands have been identified in the enamel matrix. Amelogenin (Snead et al., 1983) and amelotin (Iwasaki et al., 2005; Moffatt et al., 2006) do not possess RGD motifs or other known integrin recognition sequences. The RGD motif in enamelin it is not evolutionarily conserved (Hu et al., 1997; Nawfal et al., 2007). Ameloblastin contains binding sites for the RGD motif-binding integrins (Černý et al., 1996), and it has been shown to bind to ameloblasts, but the receptor has not yet been identified (Fukumoto et al., 2004). Ameloblasts also express bone sialoprotein that has binding sites for both hydroxyapatite and RGD-binding integrins (Ganss et al., 1999; Harris et al., 2000; Stubbs et al., 1997). Dentin sialoprotein, which also contains the RGD motif, is only transiently expressed in presecretory ameloblasts and may contribute to formation of the dentino-enamel junction rather than to enamel maturation (Bègue-Kirn et al., 1998; Paine et al., 2005).

EMD enhances the adhesion, proliferation and matrix production of fibroblast-like but not epithelial cells (Cattaneo et al., 2003; Gestrelius et al., 1997; Haase and Bartold, 2001; Hoang et al., 2000; Kawase et al., 2000). Attachment of human periodontal ligament cells to EMD is possibly mediated by bone sialoprotein as it can be inhibited by RGD-containing peptides or with an anti-αvβ3 integrin antibody (Suzuki et al., 2001). Also β1 integrins seem important to cell adhesion to EMD (van der Pauw et al., 2002). More recently, it was demonstrated that both β1 and αv integrins mediate periodontal ligament fibroblast adhesion to EMD (Narani et al., 2007). Because amelogenins do not contain any known recognition sites for integrins, it is possible that self-aggregation of amelogenins exposes cryptic integrin recognition sites. Consistently with this hypothesis, amelogenins promote binding of fibroblasts and endothelial cells via multiple integrins, including αvβ3, αvβ5 and αvβ1 (Almqvist et al., 2010; Almqvist et al., 2011). In the present study, ameloblast αvβ6 integrin did not directly bind to EMD but the cells attached via endogenously deposited matrix. Some of these matrix molecules appeared to be αvβ6 integrin ligands, such as fibronectin that readily binds to amelogenin (Narani et al., 2007). However, also *Itgb6*⁻/⁻ ameloblasts were able to attach and spread on this matrix, suggesting collaboration by other integrin receptors in ameloblast adhesion. It appears unlikely that αvβ6 integrin is essential for ameloblast cell adhesion *in vivo* either, as the ameloblasts retained their columnar shape and adhesion to the developing enamel in the *Itgb6*⁻/⁻ mice.

Amelogenin or its fragments are endocytosed by ameloblasts via a receptor-mediated mechanism involving LAMP1 and CD63 proteins (Shapiro et al., 2007). This uptake may serve as a feedback loop to upregulate amelogenin expression through stabilization of its mRNA in the cytoplasm (Xu et al., 2006). We did not find evidence for the direct involvement of αvβ6 integrin in amelogenin endocytosis. However, we found that expression of several RBMs (*Rbm26*, *Rbm45*, *Rbm8a*) was increased (4.2- to
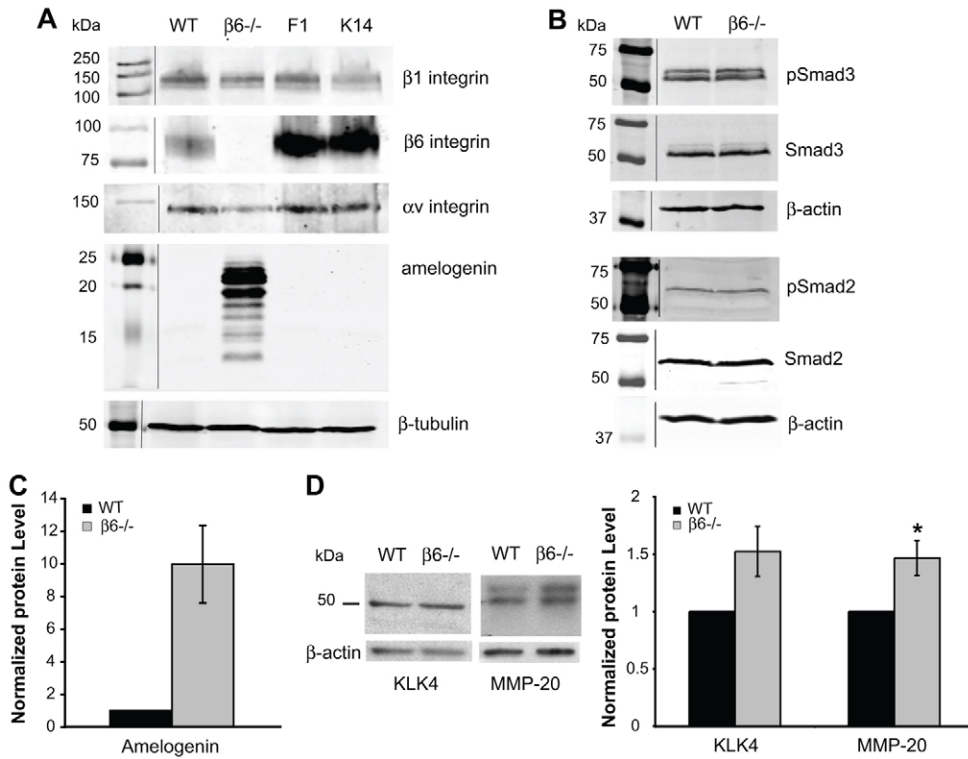
Fig. 6. Amelogenin protein is overexpressed in *Itgb6*$^{-/-}$ enamel organs. (**A**) Western blots of β1, β6 and αv integrin as well as amelogenin in WT, *Itgb6*$^{-/-}$ (β6−/−), β6 rescue (F1) and β6 overexpressing (K14) enamel organs of 3- to 6-month-old mice. (**B**) Expression and phosphorylation of pSmad2/3 in WT, *Itgb6*$^{-/-}$ enamel organs. (**C**) Normalized amelogenin expression relative to that of β-actin. (**D**) KLK4 and MMP-20 expression and quantification of western blots relative to that of β-actin. In C and D $n=3$–4 pooled samples from 4–6 mice each; mean ± s.d. is shown. *$P<0.05$.

5-fold) in the enamel organs of *Itgb6*$^{-/-}$ mice compared to WT. RBMs have been shown to critically regulate post-transcriptional RNA metabolism (Janga and Mittal, 2011). Therefore, these proteins could regulate amelogenin and enamelin mRNA stability. It is possible that the lack of αvβ6 integrin signaling in the *Itgb6*$^{-/-}$ ameloblasts may disrupt the feedback system for amelogenin expression and lead to its dysregulated accumulation in the tooth enamel by an as yet unknown mechanism.

The best-known function of αvβ6 integrin is in the activation of latent TGF-β1 (Yang et al., 2007). TGF-β and its receptors are important regulators of early tooth development (Chai et al., 1994; Chai et al., 1999; Pelton et al., 1991). In addition, TGF-β1
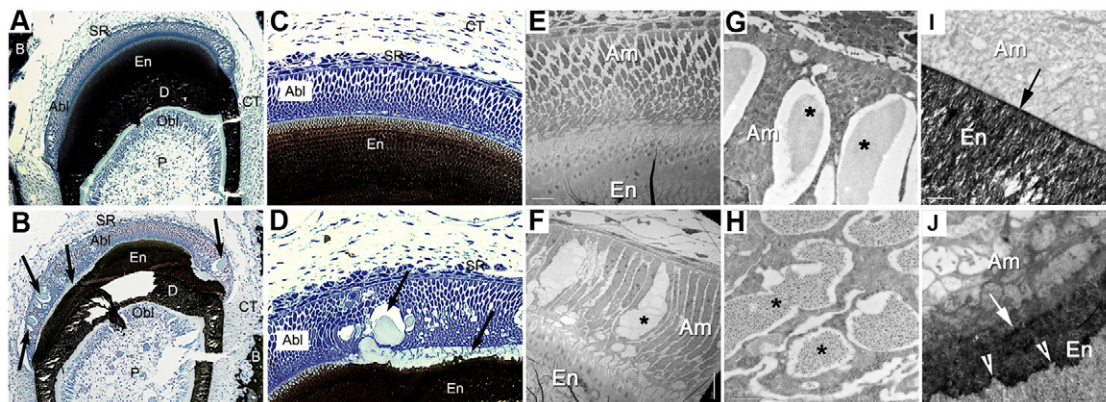

Fig. 7. Accumulation of amorphous matrix material between the ameloblast layer and the forming enamel, and between ameloblasts, in *Itgb6*$^{-/-}$ mice. (**A–D**) Undecalcified tissue sections from incisors of 14-day-old WT (A,C) and *Itgb6*$^{-/-}$ (B,D) mice stained with von Kossa reagent to detect mineralization followed by counterstaining with Toluidine Blue. Compared with WT incisors, *Itgb6*$^{-/-}$ mice show accumulation of unmineralized extracellular matrix (arrows) between the ameloblast layer and the forming enamel surface, and between individual ameloblasts. Abl, ameloblast layer; B, bone; CT, connective tissue; D, dentin; En, enamel; Obl, odontoblast layer; P, pulp tissue; SR, stellate reticulum. (**E–J**) Transmission electron micrographs of enamel organ of WT (E,I) and *Itgb6*$^{-/-}$ mice (F–H,J) showing secretory ameloblasts and enamel at the level of the second molar. Ameloblasts (Am) of the WT mouse (E) show typical organization and secretion of the enamel matrix (En) that subsequently becomes mineralized. In the *Itgb6*$^{-/-}$ ameloblast layer (F), amorphous protein pools appear in cyst-like structures between ameloblasts (asterisks) and near the enamel surface. Immunogold labeling for amelogenin of *Itgb6*$^{-/-}$ enamel organ shows abnormal amelogenin accumulation both between the cells and inside the cells (asterisks in G and H). The enamel–ameloblast (Am) interface in the WT maturation stage molar tooth is smooth and well mineralized and shows organized, parallel crystal structure at this boundary (I, arrow). In a corresponding molar crown region from an *Itgb6*$^{-/-}$ mouse, the enamel surface is less organized and irregularly mineralized with a layered appearance (J, arrow and arrowheads).
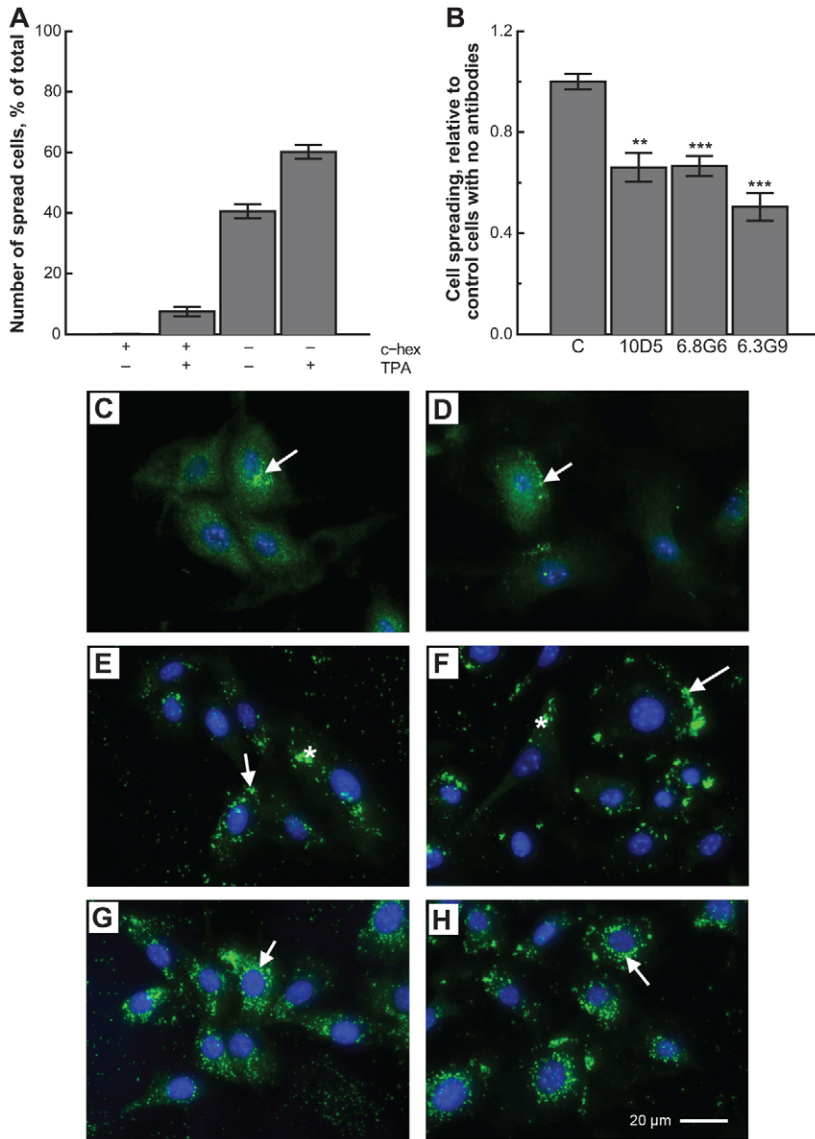
Fig. 8. Spreading, but not endocytosis, of ameloblast-like cells is regulated by αvβ6 integrin on amelogenin-rich enamel matrix. (A) Ameloblast cell spreading on plates coated with 10 mg/ml EMD in the presence or absence of 50 μM cycloheximide and 200 nM TPA. (**B**) WT ameloblast spreading on EMD in the presence of 200 nM TPA and three different anti-αvβ6 integrin antibodies (10D5, 50 μg/ml; 6.8G6, 10 μg/ml; 6.3G9, 10 μg/ml) and in the absence of cycloheximide. Control cells (C) were left untreated. Combined results of four experiments (means ± s.e.m.) are shown. **P<0.01; ***P<0.001. (**C–H**) Amelogenin endocytosis by WT (C,E,G) and $Itgb6^{-/-}$ ameloblasts (D,F,H). Both WT (C) and $Itgb6^{-/-}$ ameloblasts (D) show a very low level of endogenous amelogenin expression from immunostaining of the protein (green, arrows). Cell nuclei were counterstained with DAPI (blue). When incubated with 100 μg/ml EMD for 24 h, accumulation of amelogenin was distinct within the cells (E,F). The accumulation was seen in clusters on the cell edges (arrows) and in cytoplasmic regions (asterisks) for both cell types. In the presence of both EMD and 20 μM E64d (G,H), the staining of amelogenin became more punctate and diffuse (arrow). There was no difference in the pattern of endocytosis between $Itgb6^{-/-}$ and WT cell lines, indicating that β6 deficiency does not affect amelogenin endocytosis.

is expressed in ameloblasts of developing enamel (Gao et al., 2009). Interestingly, the tooth development in TGF-β1 mutant mice is unaffected, which could be partially due to rescue by maternal TGF-β1 (D'Souza and Litz, 1995). TGF-βs binding to type I and II TGF-β receptors (TGFβRI and TGFβRII) induces activation of Smad2/3 (Moustakas and Heldin, 2008). Human mutations in TβRI and II cause Loeys-Dietz syndrome due to abnormal receptor signaling, but no enamel phenotypes have been reported for these patients (Loeys et al., 2005). However, there is evidence that dysregulated TGF-β1 signaling may be detrimental to amelogenesis. Ameloblasts in mice overexpressing TGF-β1 under the dentin sialoprotein promoter show enamel defects, including ameloblast detachment with a pitted and hypoplastic enamel (Haruyama et al., 2006). In K14-Smad2-overexpressing mice, the ameloblast layer is disorganized and amelogenin-containing matrix is found between ameloblasts (Ito et al., 2001). No tooth abnormalities have been reported in $Smad7^{-/-}$ (an inhibitor of TGF-β signaling) mice. Mice overexpressing $Smad7$ under the K5 promoter, however, show

suppressed Smad3-mediated signaling and a failure to produce proper enamel (Helder et al., 1998; Klopcic et al., 2007). In the present study, we did not find evidence for the enamel defects in $Itgb6^{-/-}$ mice being caused by altered TGF-β1 activation. Neither phosphorylation nor the expression level of Smad2/3 was altered in the $Itgb6^{-/-}$ enamel organ. We also compared histology of enamel from $Smad3^{-/-}$ mice to that of $Itgb6^{-/-}$, and they lacked similarity (unpublished results). Previous studies have also shown that ameloblast morphology remains unaltered in $Smad3^{-/-}$ mice although the enamel is poorly mineralized due to defective protein removal at the maturation stage (Yokozeki et al., 2003). Recently, it was reported that Smad3 and FoxO1 (transcriptional co-factor for Smads) collaboratively regulate genes involved in enamel formation (Poché et al., 2012). Interestingly, in both Smad3 and FoxO1 mutant teeth, the expression of $Ambn$, $Amelx$, $Enam$, $Mmp20$ and $Klk4$ were all significantly downregulated. The fact that $Amelx$ and $Enam$ are highly upregulated in β6 integrin mutant teeth also strongly suggests that the observed enamel phenotype is not caused by

defective TGF-β1 activation. Clearly, TGF-β signaling regulates enamel formation but significant involvement of αvβ6 integrin in the activation of ameloblast TGF-βs seems unlikely.

We explored the gene expression profiles in the WT and *Itgb6*$^{-/-}$ mouse enamel organs to identify additional changes that could contribute to disturbed mineralization of *Itgb6*$^{-/-}$ mouse enamel. Interestingly, expression of *Ank* was increased in the *Itgb6*$^{-/-}$ enamel organ. ANK functions in transporting inorganic pyrophosphate to the extracellular space, where pyrophosphate serves as a potent inhibitor of extracellular matrix mineralization in calcified tissues (Harmey et al., 2004; Wang et al., 2005; Zaka and Williams, 2006). Future studies should therefore investigate whether inorganic pyrophosphate levels are increased in *Itgb6*$^{-/-}$ enamel organs, thereby contributing to the mineralization defect.

Other significant changes in gene expression observed in the *Itgb6*$^{-/-}$ enamel organ included reduced expression of arrestin *Arrdc3*, photocadherin *Pcdh21* and *Fam20B*. ARRDC3 functions in cell signaling and molecular trafficking (Rajagopal et al., 2010). It remains to be shown whether it is involved in the regulation of *Amelx* expression. Mutations in *PCDH21* cause autosomal recessive cone-rod dystrophy in the eye (Ostergaard et al., 2010), which is associated with AI in some patients, thus demonstrating possible links between retinal functions and enamel mineralization (Parry et al., 2009; Polok et al., 2009). Since cell-cell adhesion of ameloblasts via cadherins has been demonstrated to be critical for enamel mineralization (Bartlett et al., 2010), it is possible that downregulation of *Pcdh21* contributes to weakened ameloblast cell-cell adhesion and subsequent accumulation of amelogenins between the cells. FAM20B is a kinase implicated in phosphorylation and control of proteoglycans (Koike et al., 2009). It and other members of the FAM20 protein family have multiple roles in mineralized tissues. Mutations in *FAM20A* cause hypoplastic AI and gingival overgrowth (Cho et al., 2012; O'Sullivan et al., 2011), whereas FAM20C that is expressed in mineralized tissues is essential for normal bone development (Hao et al., 2007; Simpson et al., 2007; Wang et al., 2010; Ishikawa et al., 2012). FAM20B is expressed during the maturation stage of amelogenesis (O'Sullivan et al., 2011), but its function in enamel remains unknown.

Amelogenesis imperfecta represents a collection of genetic disorders that affect enamel formation both in the primary and permanent dentition in the absence of systemic manifestations (Hu et al., 2007). Mutations in several genes are associated with human AI (Hu et al., 2007; Stephanopoulos et al., 2005). In general, mutations that affect enamel matrix production (*AMELX*, *AMBN*, *ENAM*) tend to result in hypoplastic enamel while those that affect matrix removal (*MMP20*, *KLK4*) tend to result in hypomaturation of the enamel (Hu et al., 2007). Interestingly, previous studies with overexpression of normal amelogenin or its various fragments have not shown major alterations in enamel structure (Chen et al., 2003; Gibson et al., 2007; Paine et al., 2004). However, the present study clearly demonstrates that the enamel defect resulting from αvβ6 integrin deficiency and the subsequent overexpression of amelogenin and enamelin is detrimental to enamel formation and leads to a condition that mimics the hypomaturation type of AI. Therefore, *ITGB6* should be considered a candidate gene for human AI with normal thickness but altered prism structure and reduced mineralization. As discussed above, there are several putative mechanisms for how αvβ6 integrin regulates enamel biomineralization that need to be explored further.

Materials and Methods

Animals
The Animal Care Committee of the University of British Columbia approved all animal procedures used in this study. The mouse lines used were: WT (FVB background), *Itgb6*$^{-/-}$ (a generous gift from Dr Dean Sheppard, University of California, San Francisco, CA, USA), K14β6 that overexpresses human β6 integrin under the K14 promoter (Häkkinen et al., 2004) and β6 rescue mice, which were the progeny of *Itgb6*$^{-/-}$ mice bred with the K14β6 mice (F1; also from Dr Sheppard). The mice were maintained in a conventional animal care facility and had free access to standard mouse chow (Purina 5001) and water. Animals were sacrificed by CO_2 inhalation.

Western blotting
The incisors of the maxillas and mandibles of 3- to 9-month-old mice (three animals, 8–10 incisors per group) were removed, and their enamel organs scraped off with a microsurgical blade and pooled for western blotting. The antibodies used were: ameloblastin (ab72776; Abcam, Cambridge, MA, USA), amelogenin (pc-062; Kamiya Biomedical Company, Seattle, WA, USA), KLK4 (ab3636; Abcam), MMP-20 (ab76109; Abcam), Smad3 (ab28379; Abcam), pSmad3 (ab52903; Abcam), Smad2 (#3103; Cell Signaling Technology, Danvers, MA, USA), pSmad2 (#3101; Cell Signaling), β6 integrin (AF2389; R&D Systems, Inc., Minneapolis, MN, USA), αv integrin (sc-6618, Santa Cruz Biotechnology, Santa Cruz, CA, USA), β1 integrin (4080; Larjava et al., 1990), β-actin (ab8227; Abcam) and β-tubulin (mAb3408, Millipore, Temencula, MA, USA). Appropriate peroxidase-conjugated IgGs (Santa Cruz) were used as secondary antibodies. After washing, the protein bands were detected using the ECL Western Blotting Detection Kit (GE Healthcare, Baie d'Urfe, QC, Canada), and the digitized images were quantified using the ImageJ software (available at http://rsb.info.nih.gov/ij; developed by Wayne Rasband, National Institutes of Health, Bethesda, MD, USA). Alternatively, IRDye-conjugated secondary antibodies (LI-COR Biosciences, Lincoln, NE, USA) were used and the blots analyzed and quantified with an Odyssey infrared reader (LI-COR).

Gene expression profiling by microarray
The enamel organs were collected from the incisors of 6-month-old WT and *Itgb6*$^{-/-}$ mice, pooled (three animals, 8–10 incisors per group), placed into RNAlater (Ambion, Life Technologies, Inc., Burlington, ON, Canada) and stored at $-80°C$. Total RNA was extracted using either NucleoSpin RNA II or XS kit (Macherey-Nagel, Bethlehem, PA, USA) and treated with DNaseI digestion. RNA samples were analyzed using Illumina Mouse WG-6 v.2.0 Expression BeadChip at the Finnish Microarray and Sequencing Centre (Turku Centre for Biotechnology, Turku, Finland) followed by data analysis with R (R Development Core Team, 2008) and Bioconductor (Gentleman et al., 2004) softwares. The data were quantile normalized, and statistical analysis for detecting the global differences in gene expression between the groups was carried out using Bioconductor's Limma package. The chosen thresholds used in filtering the differentially expressed genes were FDR *P*-value <0.05 and absolute fold change >1.6 as the comparison cutoff.

RNA analysis by PCR
Total RNA (0.5 μg) was reverse-transcribed with SuperScript VILO cDNA Synthesis Kit (Invitrogen, Life Technologies). Real-time PCR amplification was performed on the MiniOpticon Real-Time System (Bio-Rad, Mississauga, ON, Canada) using 5 μl of RT products mixed with 10 μl of 2× iQ SYBR Green I Supermix (Bio-Rad) and 5 pmoles of primers, in a final volume of 20 μl. An amplification reaction was conducted for target genes with *Actb*, *Gapdh* and *Hprt1* as reference genes and replicated nine times for each sample. The data were analyzed based on the comparative C_T program of Gene Expression Analysis for iCycler iQ Real-Time PCR Detection System (Bio-Rad). Primer sequences (5′–3′) were: *Actb* CTTCCTTCTTGGGTATGGAATC, TAGAGGTCTTTACGGATGT-CAAC; *Ambn* CTTCCTTCTTGGGTATGGAATC, TAGAGGTCTTTACGGA-TGTCAAC; *Amelx* GCTTTTGCTATGCCCCTA, CTCATAGCTTAAGTTGA-TATAACCA; *Itgb6* AATCACCAACCCTTGCAGTAG, AATGTGCTTGAATC-CAAATGTAG; *Enam* TCTCTGCTGCCATGCCATTC, TTGATTATATCGCAT-CATCTCTTCAC; *Klk4* CATCCCTGTGGCTACCCAA, GGGCAGTTTCCCAT-TCTTTA; *Mmp20* TGCTGTGGAACTGAATGGCTA, ACACTAACCACGTC-TTCCTTC; *Hprt1* TGTTGGATTTGAAATTCCAGACAAG, CTTTTCCAGT-TTCACTAATGACACAA; *Krt14* ATCCTCTCAATTCTCCTCTGGCTC, ACCT-TGCCATCGTGCACATC; *Itgb1* GCTGGTTCTATTTCACCTATTCA, CAAC-CACGCCTGCTACAA; *Itgb4* CCAGCTGAGACCAATGGCGA, GAGCACCTT-CTTCATAGGTCCA; *Gapdh* CTTTGTCAAGCTCATTTCCTGGTA, GGCCA-TGAGGTCCACCA.

Attrition rate
Maxillas and mandibles of 3- to 24-month-old WT and *Itgb6*$^{-/-}$ mice were defleshed mechanically and with 2% KOH (EM Science, Merck, Darmstadt, Germany). Attrition of the molars was scored based on cusp heights where 0=<10% attrition of the cusps, 1=attrition reaching up to 50% of the cusp height,

and 2=more than 50% attrition. In a cross-sectional study, we also compared the attrition rate of molars in 6-month-old WT, $Itgb6^{-/-}$, K14-β6 and rescue mice.

Scanning electron microscopy
Calcium-to-phosphorus ratio
WT and $Itgb6^{-/-}$ mice (11- to 14-months old) were sacrificed, decapitated and their heads were fixed in 4% formaldehyde in phosphate-buffered saline (PBSp; pH 7.2). The mandibles were dissected and further fixed in 2.5% glutaraldehyde for 1 h at 4°C. The samples were post-fixed with 1 M OsO_4 for 1 h at RT. After three rinses, the specimens were dehydrated, critical-point dried, gold-coated and viewed by scanning electron microscopy (SEM). Three standardized areas (mesial, middle and distal) on the mid-lingual surface of the third molar were used to measure calcium-to-phosphorus ratios using energy dispersive X-ray spectroscopy (Hitachi S-3000N SEM with light element EDX).

Visualization of prism structures
Defleshed and dried incisors from WT and $Itgb6^{-/-}$ mice were frozen by immersion in liquid nitrogen and then fractured (along the line from root to crown) with a pre-cooled scalpel blade. The fractured portion of the incisor was treated at RT in 35% phosphoric acid for 30 s, rinsed and air-dried (Sánchez-Quevedo et al., 2006). The incisors were then mounted and coated with a 10 nm layer of gold/palladium. Each sample was imaged by SEM with identical imaging conditions at 4 kV.

Immunohistochemistry
Immunostaining of β6 integrin was performed on frozen sections (6 μm) of the secretory stage of an upper incisor and a developing upper molar from a 3-day-old WT mouse using the β6 integrin antibody β6B1 (a generous gift from Dr Dean Sheppard).

Impacted human third molars containing the dental follicle were collected anonymously from patients requiring extractions of these teeth as a part of their treatment (approved by the Clinical Research Ethics Board, University of British Columbia). Teeth with soft tissue remaining were fixed with 2% formaldehyde in PBS and then decalcified in the same fixative containing 0.4 M EDTA. Frozen sections (6 μm) containing patches of cells resembling ameloblasts were identified and used for immunolocalization of K14 (MCA890; AbD Serotec, Oxford, UK), amelogenin and β6 integrin as described above using a fluorescently-labeled secondary antibody (Alexa Fluor 488; Invitrogen).

Mineral analysis of incisors
Hemi-maxillas and -mandibles from 7-week-old male and female WT and $Itgb6^{-/-}$ mice were removed and cleaned of adhering soft tissues. Procedures employed for isolating and removing sequential 1-mm-long strips of developing enamel from maxillary and mandibular incisors have been described in detail previously (Smith et al., 2005; Smith et al., 2009; Smith et al., 2011). Directly measured 'before' and 'after' heating weights were used to calculate various parameters including mineral-to-volatiles ratio, which represents the after-heating weight (mineral content of sample) divided by the difference between the initial dry weight minus the after-heating weight (amount of volatiles in sample; mostly protein). Weight data for enamel strips were collected from a minimum of nine maxillary and nine mandibular samples per genotype.

In situ hybridization
Jaws from 10-day-old mice were fixed in 4% paraformaldehyde, decalcified for 24 h using Morse's solution (Nakatomi et al., 2006) and then embedded in paraffin. Sections (5 μm) were treated with proteinase K at 7 μg/ml in PBS for 25 min, postfixed with paraformaldehyde and then treated with 0.2 M HCl for 10 min prior to the hybridization using digoxigenin–UTP-labeled riboprobes as previously described (Yoshida et al., 2010). A plasmid for integrin β6 integrin riboprobe was generated by inserting PCR products from mouse cDNA into pCRII-TOPO vector (Invitrogen). Primers used for the PCR were 5′: AGGGGTGACTGCTATTGTGG and 3′: GGCACCAATGCTTTACACT.

Undecalcified histology, transmission electron microscopy and immunogold labeling
WT and $Itgb6^{-/-}$ mouse mandibles were immersion-fixed overnight in sodium-cacodylate-buffered aldehyde solution and cut into segments containing the molars, underlying incisor and surrounding alveolar bone. The samples were dehydrated through a graded ethanol series and infiltrated in acrylic resin (LR White; London Resin Company, Berkshire, UK) followed by polymerization of at 55°C for 2 days. 1-μm sections of hemi-mandibles were cut with a diamond knife using an ultramicrotome, and glass slide-mounted sections were stained with 1% Toluidine Blue and von Kossa reagent to detect mineralization. Immunogold labeling for amelogenin coupled with TEM was performed as described previously (McKee and Nanci, 1995; McKee et al., 1996) using an anti-amelogenin antibody kindly provided by Dr Takashi Uchida of Hiroshima University, Japan (Uchida et al., 1991).

Micro-computed tomography
Micro-computed tomography (Micro-CT, model 1072; Skyscan, Kontich, Belgium) of undecalcified hemi-mandibles was performed at the level of the first molar from three samples of each genotype. The X-ray source was operated at maximum power (80 KeV) and at 100 μA. Images were captured using a 12-bit, cooled, charge-coupled device camera (1024×1024 pixels) coupled by a fiber optic taper to the scintillator. Using a rotation step of 0.9°, total scanning time was 35 min for each sample with a scan resolution of 5 μm, after which ~300 sections (slice-to-slice distance of 16.5 μm) were reconstructed using Skyscan tomography software. Appropriate imaging planes were selected to show three-dimensional longitudinal and cross-sectional 'sections' (segments) of the first molar and underlying incisor.

Establishment of ameloblast cell lines
Maxillary and mandibular incisors of 5- to 6-month-old WT and $Itgb6^{-/-}$ mice were prepared under aseptic conditions and placed in cell culture wells pre-coated with bovine fibronectin (10 μg/ml; Millipore) and collagen (30 μg/ml; PureCol®; Advanced BioMatrix, Inc., San Diego, CA, USA) in keratinocyte growth medium (KCM) (Häkkinen et al., 2001). The cells growing out from the explants were differentially trypsinized to selectively remove the more easily released fibroblastic cells. The remaining epitheloid cells were confirmed to express ameloblast marker K14 as well as to be positive (WT) or negative ($Itgb6^{-/-}$) for β6 integrin expression by PCR. The ameloblasts were routinely grown in KCM.

Cell spreading assays
For cell spreading assays, WT ameloblasts were seeded in plates coated with EMD (10,000 μg/ml in 10 mM acetic acid; Emdogain®, Straumann, Basel, Switzerland) in triplicates in the presence or absence of 50 μM cycloheximide (a protein synthesis blocker) and 200 nM TPA (an integrin activator). Cell spreading was quantified as described previously (Narani et al., 2007).

To explore the role of αvβ6 integrin in cell spreading on EMD, WT or $Itgb6^{-/-}$ ameloblasts were pre-incubated on ice with anti-integrin antibodies and then allowed to spread on EMD in the presence of TPA and in the absence of cycloheximide. The anti-αvβ6 integrin antibodies used were: MAB2077Z (50 μg/ml; Millipore), 6.8G6 (10 μg/ml; Biogen Idec, Cambridge, MA, USA) (Weinreb et al., 2004) and 6.3G9 (10 μg/ml; Biogen).

Amelogenin endocytosis by ameloblast-like cells
WT and $Itgb6^{-/-}$ ameloblasts were seeded onto glass coverslips (10,000 cells per ml) for 24 h in KCM. The cells were treated with KCM only, with 100 μg/ml of EMD or pre-treated for 10 min with 20 μM E64d [(2S,3S)-*trans*-epoxysuccinyl-L-leucylamido-3-methylbutane ethyl ester; inhibits lysosomal degradation of endocytosed proteins (McGowan et al., 1989)], followed by addition of 100 μg/ml of EMD. The cells were then incubated for 24 h and processed for immunofluorescence staining with anti-amelogenin antibody (PC-062).

Statistical analysis
The experiments were repeated at least three times. The difference between WT and $Itgb6^{-/-}$ mice was calculated using unpaired, two-tailed Student's *t*-test using GraphPad InStat 3 software. Multiple comparison tests were performed using one-way ANOVA with Tukey's post-test. Statistical significance was set at $P<0.05$.

Author Contributions
L.M. collected and analyzed most of the data and wrote a large part of the manuscript; L. Koivisto assisted in western blotting and cell spreading experiments and manuscript writing; G.J. performed real-time PCR analyses; L. Kytömäki performed and analyzed the gene arrays; M.H. and C.W. assisted in collecting samples for immunohistochemistry; G.R.O. assisted in endocytosis experiments; Y.X. assisted in immunolocalization studies; K.H. provided samples and assisted in manuscript writing; T.Y. performed in situ hybridization experiments; C.E.S. analyzed the mineral and protein contents of enamel; J.H. assisted in gene profiling and manuscript writing; L.H. participated in experiment planning and manuscript writing; M.D.M. performed hard tissue sectioning and EM studies and assisted in manuscript writing; H.L. supervised all experiments and participated in manuscript writing.

References

Almqvist, S., Werthén, M., Johansson, A., Agren, M. S., Thomsen, P. and Lyngstadaas, S. P. (2010). Amelogenin is phagocytized and induces changes in integrin configuration, gene expression and proliferation of cultured normal human dermal fibroblasts. *J. Mater. Sci. Mater. Med.* **21**, 947-954.

Almqvist, S., Werthen, M., Lyngstadaas, S. P., Gretzer, C. and Thomsen, P. (2011). Amelogenins promote an alternatively activated macrophage phenotype in vitro. *Int. J. Nano Biomaterials.* **3**, 282-298.

Bartlett, J. D., Simmer, J. P., Xue, J., Margolis, H. C. and Moreno, E. C. (1996). Molecular cloning and mRNA tissue distribution of a novel matrix metalloproteinase isolated from porcine enamel organ. *Gene* **183**, 123-128.

Bartlett, J. D., Dobeck, J. M., Tye, C. E., Perez-Moreno, M., Stokes, N., Reynolds, A. B., Fuchs, E. and Skobe, Z. (2010). Targeted p120-catenin ablation disrupts dental enamel development. *PLoS ONE* **5**, e12703.

Bègue-Kirn, C., Krebsbach, P. H., Bartlett, J. D. and Butler, W. T. (1998). Dentin sialoprotein, dentin phosphoprotein, enamelysin and ameloblastin: tooth-specific molecules that are distinctively expressed during murine dental differentiation. *Eur. J. Oral Sci.* **106**, 963-970.

Breuss, J. M., Gillett, N., Lu, L., Sheppard, D. and Pytela, R. (1993). Restricted distribution of integrin β 6 mRNA in primate epithelial tissues. *J. Histochem. Cytochem.* **41**, 1521-1527.

Cattaneo, V., Rota, C., Silvestri, M., Piacentini, C., Forlino, A., Gallanti, A., Rasperini, G. and Cetta, G. (2003). Effect of enamel matrix derivative on human periodontal fibroblasts: proliferation, morphology and root surface colonization. An in vitro study. *J. Periodontal Res.* **38**, 568-574.

Černý, R., Slaby, I., Hammarström, L. and Wurtz, T. (1996). A novel gene expressed in rat ameloblasts codes for proteins with cell binding domains. *J. Bone Miner. Res.* **11**, 883-891.

Chai, Y., Mah, A., Crohin, C., Groff, S., Bringas, P., Jr, Le, T., Santos, V. and Slavkin, H. C. (1994). Specific transforming growth factor-β subtypes regulate embryonic mouse Meckel's cartilage and tooth development. *Dev. Biol.* **162**, 85-103.

Chai, Y., Zhao, J., Mogharei, A., Xu, B., Bringas, P., Jr, Shuler, C. and Warburton, D. (1999). Inhibition of transforming growth factor-β type II receptor signaling accelerates tooth formation in mouse first branchial arch explants. *Mech. Dev.* **86**, 63-74.

Chen, E., Yuan, Z. A., Wright, J. T., Hong, S. P., Li, Y., Collier, P. M., Hall, B., D'Angelo, M., Decker, S., Piddington, R. et al. (2003). The small bovine amelogenin LRAP fails to rescue the amelogenin null phenotype. *Calcif. Tissue Int.* **73**, 487-495.

Cho, S. H., Seymen, F., Lee, K. E., Lee, S. K., Kweon, Y. S., Kim, K. J., Jung, S. E., Song, S. J., Yildirim, M., Bayram, M. et al. (2012). Novel FAM20A mutations in hypoplastic amelogenesis imperfecta. *Hum. Mutat.* **33**, 91-94.

Crawford, P. J., Aldred, M. and Bloch-Zupan, A. (2007). Amelogenesis imperfecta. *Orphanet J. Rare Dis.* **2**, 17.

D'Souza, R. N. and Litz, M. (1995). Analysis of tooth development in mice bearing a TGF-β 1 null mutation. *Connect. Tissue Res.* **32**, 41-46.

Eastoe, J. E. (1979). Enamel protein chemistry—past, present and future. *J. Dent. Res.* **58 Spec. Issue B**, 753-764.

Fukumoto, S., Kiba, T., Hall, B., Iehara, N., Nakamura, T., Longenecker, G., Krebsbach, P. H., Nanci, A., Kulkarni, A. B. and Yamada, Y. (2004). Ameloblastin is a cell adhesion molecule required for maintaining the differentiation state of ameloblasts. *J. Cell Biol.* **167**, 973-983.

Ganss, B., Kim, R. H. and Sodek, J. (1999). Bone sialoprotein. *Crit. Rev. Oral Biol. Med.* **10**, 79-98.

Gao, Y., Li, D., Han, T., Sun, Y. and Zhang, J. (2009). TGF-β1 and TGFBR1 are expressed in ameloblasts and promote MMP20 expression. *Anat. Rec. (Hoboken)* **292**, 885-890.

Gentleman, R. C., Carey, V. J., Bates, D. M., Bolstad, B., Dettling, M., Dudoit, S., Ellis, B., Gautier, L., Ge, Y., Gentry, J. et al. (2004). Bioconductor: open software development for computational biology and bioinformatics. *Genome Biol.* **5**, R80.

Gestrelius, S., Andersson, C., Lidström, D., Hammarström, L. and Somerman, M. (1997). In vitro studies on periodontal ligament cells and enamel matrix derivative. *J. Clin. Periodontol.* **24**, 685-692.

Ghannad, F., Nica, D., Fulle, M. I., Grenier, D., Putnins, E. E., Johnston, S., Eslami, A., Koivisto, L., Jiang, G., McKee, M. D. et al. (2008). Absence of alphavbeta6 integrin is linked to initiation and progression of periodontal disease. *Am. J. Pathol.* **172**, 1271-1286.

Gibson, C. W., Yuan, Z. A., Li, Y., Daly, B., Suggs, C., Aragon, M. A., Alawi, F., Kulkarni, A. B. and Wright, J. T. (2007). Transgenic mice that express normal and mutated amelogenins. *J. Dent. Res.* **86**, 331-335.

Haase, H. R. and Bartold, P. M. (2001). Enamel matrix derivative induces matrix synthesis by cultured human periodontal fibroblast cells. *J. Periodontol.* **72**, 341-348.

Hahm, K., Lukashev, M. E., Luo, Y., Yang, W. J., Dolinski, B. M., Weinreb, P. H., Simon, K. J., Chun Wang, L., Leone, D. R., Lobb, R. R. et al. (2007). Alphav β6 integrin regulates renal fibrosis and inflammation in Alport mouse. *Am. J. Pathol.* **170**, 110-125.

Häkkinen, L., Koivisto, L. and Larjava, H. (2001). An improved method for culture of epidermal keratinocytes from newborn mouse skin. *Methods Cell Sci.* **23**, 189-196.

Häkkinen, L., Koivisto, L., Gardner, H., Saarialho-Kere, U., Carroll, J. M., Lakso, M., Rauvala, H., Laato, M., Heino, J. and Larjava, H. (2004). Increased expression of β6-integrin in skin leads to spontaneous development of chronic wounds. *Am. J. Pathol.* **164**, 229-242.

Hao, J., Narayanan, K., Muni, T., Ramachandran, A. and George, A. (2007). Dentin matrix protein 4, a novel secretory calcium-binding protein that modulates odontoblast differentiation. *J. Biol. Chem.* **282**, 15357-15365.

Harmey, D., Hessle, L., Narisawa, S., Johnson, K. A., Terkeltaub, R. and Millán, J. L. (2004). Concerted regulation of inorganic pyrophosphate and osteopontin by akp2, enpp1, and ank: an integrated model of the pathogenesis of mineralization disorders. *Am. J. Pathol.* **164**, 1199-1209.

Harris, N. L., Rattray, K. R., Tye, C. E., Underhill, T. M., Somerman, M. J., D'Errico, J. A., Chambers, A. F., Hunter, G. K. and Goldberg, H. A. (2000). Functional analysis of bone sialoprotein: identification of the hydroxyapatite-nucleating and cell-binding domains by recombinant peptide expression and site-directed mutagenesis. *Bone* **27**, 795-802.

Haruyama, N., Thyagarajan, T., Skobe, Z., Wright, J. T., Septier, D., Sreenath, T. L., Goldberg, M. and Kulkarni, A. B. (2006). Overexpression of transforming growth factor-β1 in teeth results in detachment of ameloblasts and enamel defects. *Eur. J. Oral Sci.* **114 Suppl. 1**, 30-34, discussion 39-41, 379.

Helder, M. N., Karg, H., Bervoets, T. J., Vukicevic, S., Burger, E. H., D'Souza, R. N., Wöltgens, J. H., Karsenty, G. and Bronckers, A. L. (1998). Bone morphogenetic protein-7 (osteogenic protein-1, OP-1) and tooth development. *J. Dent. Res.* **77**, 545-554.

Hoang, A. M., Oates, T. W. and Cochran, D. L. (2000). In vitro wound healing responses to enamel matrix derivative. *J. Periodontol.* **71**, 1270-1277.

Horan, G. S., Wood, S., Ona, V., Li, D. J., Lukashev, M. E., Weinreb, P. H., Simon, K. J., Hahm, K., Allaire, N. E., Rinaldi, N. J. et al. (2008). Partial inhibition of integrin α(ν)β6 prevents pulmonary fibrosis without exacerbating inflammation. *Am. J. Respir. Crit. Care Med.* **177**, 56-65.

Hu, C. C., Fukae, M., Uchida, T., Qian, Q., Zhang, C. H., Ryu, O. H., Tanabe, T., Yamakoshi, Y., Murakami, C., Dohi, N. et al. (1997). Cloning and characterization of porcine enamelin mRNAs. *J. Dent. Res.* **76**, 1720-1729.

Hu, J. C., Chun, Y. H., Al Hazzazzi, T. and Simmer, J. P. (2007). Enamel formation and amelogenesis imperfecta. *Cells Tissues Organs* **186**, 78-85.

Hynes, R. O. (2004). The emergence of integrins: a personal and historical perspective. *Matrix Biol.* **23**, 333-340.

Ishikawa, H. O., Xu, A., Ogura, E., Manning, G. and Irvine, K. D. (2012). The Raine syndrome protein FAM20C is a Golgi kinase that phosphorylates bio-mineralization proteins. *PLoS ONE* **7**, e42988.

Ito, Y., Sarkar, P., Mi, Q., Wu, N., Bringas, P., Jr, Liu, Y., Reddy, S., Maxson, R., Deng, C. and Chai, Y. (2001). Overexpression of Smad2 reveals its concerted action with Smad4 in regulating TGF-beta-mediated epidermal homeostasis. *Dev. Biol.* **236**, 181-194.

Iwasaki, K., Bajenova, E., Somogyi-Ganss, E., Miller, M., Nguyen, V., Nourkeyhani, H., Gao, Y., Wendel, M. and Ganss, B. (2005). Amelotin – a novel secreted, ameloblast-specific protein. *J. Dent. Res.* **84**, 1127-1132.

Janga, S. C. and Mittal, N. (2011). Construction, structure and dynamics of post-transcriptional regulatory network directed by RNA-binding proteins. *Adv. Exp. Med. Biol.* **722**, 103-117.

Kawase, T., Okuda, K., Yoshie, H. and Burns, D. M. (2000). Cytostatic action of enamel matrix derivative (EMDOGAIN) on human oral squamous cell carcinoma-derived SCC25 epithelial cells. *J. Periodontal Res.* **35**, 291-300.

Klopcic, B., Maass, T., Meyer, E., Lehr, H. A., Metzger, D., Chambon, P., Mann, A. and Blessing, M. (2007). TGF-β superfamily signaling is essential for tooth and hair morphogenesis and differentiation. *Eur. J. Cell Biol.* **86**, 781-799.

Koike, T., Izumikawa, T., Tamura, J. and Kitagawa, H. (2009). FAM20B is a kinase that phosphorylates xylose in the glycosaminoglycan-protein linkage region. *Biochem. J.* **421**, 157-162.

Krebsbach, P. H., Lee, S. K., Matsuki, Y., Kozak, C. A., Yamada, K. M. and Yamada, Y. (1996). Full-length sequence, localization, and chromosomal mapping of ameloblastin. A novel tooth-specific gene. *J. Biol. Chem.* **271**, 4431-4435.

Larjava, H., Peltonen, J., Akiyama, S. K., Yamada, S. S., Gralnick, H. R., Uitto, J. and Yamada, K. M. (1990). Novel function for β 1 integrins in keratinocyte cell-cell interactions. *J. Cell Biol.* **110**, 803-815.

Larjava, H., Koivisto, L., Häkkinen, L. and Heino, J. (2011). Epithelial integrins with special reference to oral epithelia. *J. Dent. Res.* **90**, 1367-1376.

Loeys, B. L., Chen, J., Neptune, E. R., Judge, D. P., Podowski, M., Holm, T., Meyers, J., Leitch, C. C., Katsanis, N., Sharifi, N. et al. (2005). A syndrome of altered cardiovascular, craniofacial, neurocognitive and skeletal development caused by mutations in TGFBR1 or TGFBR2. *Nat. Genet.* **37**, 275-281.

McGowan, E. B., Becker, E. and Detwiler, T. C. (1989). Inhibition of calpain in intact platelets by the thiol protease inhibitor E-64d. *Biochem. Biophys. Res. Commun.* **158**, 432-435.

McKee, M. D. and Nanci, A. (1995). Osteopontin and the bone remodeling sequence. Colloidal-gold immunocytochemistry of an interfacial extracellular matrix protein. *Ann. N. Y. Acad. Sci.* **760**, 177-189.

McKee, M. D., Zalzal, S. and Nanci, A. (1996). Extracellular matrix in tooth cementum and mantle dentin: localization of osteopontin and other noncollagenous proteins, plasma proteins, and glycoconjugates by electron microscopy. *Anat. Rec.* **245**, 293-312.

Moffatt, P., Smith, C. E., Sooknanan, R., St-Arnaud, R. and Nanci, A. (2006). Identification of secreted and membrane proteins in the rat incisor enamel organ using a signal-trap screening approach. *Eur. J. Oral Sci.* **114 Suppl. 1**, 139-146, discussion 164-165, 380-381.

Moustakas, A. and Heldin, C. H. (2008). Dynamic control of TGF-β signaling and its links to the cytoskeleton. *FEBS Lett.* **582**, 2051-2065.

Munger, J. S., Huang, X., Kawakatsu, H., Griffiths, M. J., Dalton, S. L., Wu, J., Pittet, J. F., Kaminski, N., Garat, C., Matthay, M. A. et al. (1999). The integrin α v β 6 binds and activates latent TGF β 1: a mechanism for regulating pulmonary inflammation and fibrosis. *Cell* **96**, 319-328.

Nakatomi, M., Morita, I., Eto, K. and Ota, M. S. (2006). Sonic hedgehog signaling is important in tooth root development. *J. Dent. Res.* **85**, 427-431.

Nanci, A. and Smith, C. E. (2000). Matrix-mediated mineralization in enamel and the collagen-based hard tissues. In *Intl. Con. on Chem. Biol. Min. Tis.* (ed. N. Goldberg, A. Boskey and C. Robinson), pp. 217-224. Am. Acad. Orthoped. Surg.

Narani, N., Owen, G. R., Häkkinen, L., Putnins, E. and Larjava, H. (2007). Enamel matrix proteins bind to wound matrix proteins and regulate their cell-adhesive properties. *Eur. J. Oral Sci.* **115**, 288-295.

Nawfal, A.-H., Sidney, D. and Sire, J.-Y. (2007). Mammalian enamelins: identification of conserved regions, evolution mode and made use of for validation of mutations leading to amelogenesis imperfecta. *Eur. Cell. Mater.* **14**, 67.

O'Sullivan, J., Bitu, C. C., Daly, S. B., Urquhart, J. E., Barron, M. J., Bhaskar, S. S., Martelli-Júnior, H., dos Santos Neto, P. E., Mansilla, M. A., Murray, J. C. et al. (2011). Whole-Exome sequencing identifies FAM20A mutations as a cause of amelogenesis imperfecta and gingival hyperplasia syndrome. *Am. J. Hum. Genet.* **88**, 616-620.

Ostergaard, E., Batbayli, M., Duno, M., Vilhelmsen, K. and Rosenberg, T. (2010). Mutations in PCDH21 cause autosomal recessive cone-rod dystrophy. *J. Med. Genet.* **47**, 665-669.

Paine, M. L., Zhu, D. H., Luo, W. and Snead, M. L. (2004). Overexpression of TRAP in the enamel matrix does not alter the enamel structural hierarchy. *Cells Tissues Organs* **176**, 7-16.

Paine, M. L., Luo, W., Wang, H. J., Bringas, P., Jr, Ngan, A. Y., Miklus, V. G., Zhu, D. H., MacDougall, M., White, S. N. and Snead, M. L. (2005). Dentin sialoprotein and dentin phosphoprotein overexpression during amelogenesis. *J. Biol. Chem.* **280**, 31991-31998.

Parry, D. A., Mighell, A. J., El-Sayed, W., Shore, R. C., Jalili, I. K., Dollfus, H., Bloch-Zupan, A., Carlos, R., Carr, I. M., Downey, L. M. et al. (2009). Mutations in CNNM4 cause Jalili syndrome, consisting of autosomal-recessive cone-rod dystrophy and amelogenesis imperfecta. *Am. J. Hum. Genet.* **84**, 266-273.

Patsenker, E., Popov, Y., Stickel, F., Jonczyk, A., Goodman, S. L. and Schuppan, D. (2008). Inhibition of integrin alphavbeta6 on cholangiocytes blocks transforming growth factor-β activation and retards biliary fibrosis progression. *Gastroenterology* **135**, 660-670.

Pelton, R. W., Saxena, B., Jones, M., Moses, H. L. and Gold, L. I. (1991). Immunohistochemical localization of TGF β 1, TGF β 2, and TGF β 3 in the mouse embryo: expression patterns suggest multiple roles during embryonic development. *J. Cell Biol.* **115**, 1091-1105.

Poché, R. A., Sharma, R., Garcia, M. D., Wada, A. M., Nolte, M. J., Udan, R. S., Paik, J. H., DePinho, R. A., Bartlett, J. D. and Dickinson, M. E. (2012). Transcription factor FoxO1 is essential for enamel biomineralization. *PLoS ONE* **7**, e30357.

Polok, B., Escher, P., Ambresin, A., Chouery, E., Bolay, S., Meunier, I., Nan, F., Hamel, C., Munier, F. L., Thilo, B. et al. (2009). Mutations in CNNM4 cause recessive cone-rod dystrophy with amelogenesis imperfecta. *Am. J. Hum. Genet.* **84**, 259-265.

R Development Core Team (2008). *R: A Language and Environment for Statistical Computing.* ISBN 3-900051-07-0. Vienna, Austria: R Foundation for Statistical Computing.

Rajagopal, S., Rajagopal, K. and Lefkowitz, R. J. (2010). Teaching old receptors new tricks: biasing seven-transmembrane receptors. *Nat. Rev. Drug Discov.* **9**, 373-386.

Salmivirta, K., Gullberg, D., Hirsch, E., Altruda, F. and Ekblom, P. (1996). Integrin subunit expression associated with epithelial-mesenchymal interactions during murine tooth development. *Dev. Dyn.* **205**, 104-113.

Sánchez-Quevedo, C., Ceballos, G., Rodríguez, I. A., García, J. M. and Alaminos, M. (2006). Acid-etching effects in hypomineralized amelogenesis imperfecta. A microscopic and microanalytical study. *Med. Oral Patol. Oral Cir. Bucal* **11**, E40-E43.

Schroeder, H. E. and Listgarten, M. A. (1977). Fine structure of the developing epithelial attachment of human teeth. In *Monographs in Developmental Biology*, vol. 2, revision of 1971 edition (ed. A. Wolsky). Basel: S. Karger AG.

Shapiro, J. L., Wen, X., Okamoto, C. T., Wang, H. J., Lyngstadaas, S. P., Goldberg, M., Snead, M. L. and Paine, M. L. (2007). Cellular uptake of amelogenin, and its localization to CD63, and Lamp1-positive vesicles. *Cell. Mol. Life Sci.* **64**, 244-256.

Simmer, J. P., Papagerakis, P., Smith, C. E., Fisher, D. C., Rountrey, A. N., Zheng, L. and Hu, J. C.-C. (2010). Regulation of dental enamel shape and hardness. *J. Dent. Res.* **89**, 1024-1038.

Simpson, M. A., Hsu, R., Keir, L. S., Hao, J., Sivapalan, G., Ernst, L. M., Zackai, E. H., Al-Gazali, L. I., Hulskamp, G., Kingston, H. M. et al. (2007). Mutations in FAM20C are associated with lethal osteosclerotic bone dysplasia (Raine syndrome), highlighting a crucial molecule in bone development. *Am. J. Hum. Genet.* **81**, 906-912.

Smith, C. E., Chong, D. L., Bartlett, J. D. and Margolis, H. C. (2005). Mineral acquisition rates in developing enamel on maxillary and mandibular incisors of rats and mice: implications to extracellular acid loading as apatite crystals mature. *J. Bone Miner. Res.* **20**, 240-249.

Smith, C. E., Wazen, R., Hu, Y., Zalzal, S. F., Nanci, A., Simmer, J. P. and Hu, J. C. (2009). Consequences for enamel development and mineralization resulting from loss of function of ameloblastin or enamelin. *Eur. J. Oral Sci.* **117**, 485-497.

Smith, C. E., Richardson, A. S., Hu, Y., Bartlett, J. D., Hu, J. C. and Simmer, J. P. (2011). Effect of kallikrein 4 loss on enamel mineralization: comparison with mice lacking matrix metalloproteinase 20. *J. Biol. Chem.* **286**, 18149-18160.

Snead, M. L., Zeichner-David, M., Chandra, T., Robson, K. J., Woo, S. L. and Slavkin, H. C. (1983). Construction and identification of mouse amelogenin cDNA clones. *Proc. Natl. Acad. Sci. USA* **80**, 7254-7258.

Stephanopoulos, G., Garefalaki, M. E. and Lyroudia, K. (2005). Genes and related proteins involved in amelogenesis imperfecta. *J. Dent. Res.* **84**, 1117-1126.

Stubbs, J. T., 3rd, Mintz, K. P., Eanes, E. D., Torchia, D. A. and Fisher, L. W. (1997). Characterization of native and recombinant bone sialoprotein: delineation of the mineral-binding and cell adhesion domains and structural analysis of the RGD domain. *J. Bone Miner. Res.* **12**, 1210-1222.

Suzuki, N., Ohyama, M., Maeno, M., Ito, K. and Otsuka, K. (2001). Attachment of human periodontal ligament cells to enamel matrix-derived protein is mediated via interaction between BSP-like molecules and integrin α(v)β3. *J. Periodontol.* **72**, 1520-1526.

Uchida, T., Tanabe, T., Fukae, M., Shimizu, M., Yamada, M., Miake, K. and Kobayashi, S. (1991). Immunochemical and immunohistochemical studies, using antisera against porcine 25 kDa amelogenin, 89 kDa enamelin and the 13-17 kDa nonamelogenins, on immature enamel of the pig and rat. *Histochemistry* **96**, 129-138.

van der Pauw, M. T., Everts, V. and Beertsen, W. (2002). Expression of integrins by human periodontal ligament and gingival fibroblasts and their involvement in fibroblast adhesion to enamel matrix-derived proteins. *J. Periodontal Res.* **37**, 317-323.

Wang, W., Xu, J., Du, B. and Kirsch, T. (2005). Role of the progressive ankylosis gene (ank) in cartilage mineralization. *Mol. Cell. Biol.* **25**, 312-323.

Wang, X., Hao, J., Xie, Y., Sun, Y., Hernandez, B., Yamoah, A. K., Prasad, M., Zhu, Q., Feng, J. Q. and Qin, C. (2010). Expression of FAM20C in the osteogenesis and odontogenesis of mouse. *J. Histochem. Cytochem.* **58**, 957-967.

Weinreb, P. H., Simon, K. J., Rayhorn, P., Yang, W. J., Leone, D. R., Dolinski, B. M., Pearse, B. R., Yokota, Y., Kawakatsu, H., Atakilit, A. et al. (2004). Function-blocking integrin alphavbeta6 monoclonal antibodies: distinct ligand-mimetic and nonligand-mimetic classes. *J. Biol. Chem.* **279**, 17875-17887.

Wright, J. T. (2010). Oral manifestations in the epidermolysis bullosa spectrum. *Dermatol. Clin.* **28**, 159-164.

Wu, J. E. and Santoro, S. A. (1994). Complex patterns of expression suggest extensive roles for the α 2 β 1 integrin in murine development. *Dev. Dyn.* **199**, 292-314.

Xu, L., Harada, H., Yokohama-Tamaki, T., Matsumoto, S., Tanaka, J. and Taniguchi, A. (2006). Reuptake of extracellular amelogenin by dental epithelial cells results in increased levels of amelogenin mRNA through enhanced mRNA stabilization. *J. Biol. Chem.* **281**, 2257-2262.

Yamada, S., Yamada, K. M. and Brown, K. E. (1994). Integrin regulatory switching in development: oscillation of β 5 integrin mRNA expression during epithelial-mesenchymal interactions in tooth development. *Int. J. Dev. Biol.* **38**, 553-556.

Yang, Z., Mu, Z., Dabovic, B., Jurukovski, V., Yu, D., Sung, J., Xiong, X. and Munger, J. S. (2007). Absence of integrin-mediated TGFbeta1 activation in vivo recapitulates the phenotype of TGFbeta1-null mice. *J. Cell Biol.* **176**, 787-793.

Yokozeki, M., Afanador, E., Nishi, M., Kaneko, K., Shimokawa, H., Yokote, K., Deng, C., Tsuchida, K., Sugino, H. and Moriyama, K. (2003). Smad3 is required for enamel biomineralization. *Biochem. Biophys. Res. Commun.* **305**, 684-690.

Yoshida, T., Miyoshi, J., Takai, Y. and Thesleff, I. (2010). Cooperation of nectin-1 and nectin-3 is required for normal ameloblast function and crown shape development in mouse teeth. *Dev. Dyn.* **239**, 2558-2569.

Zaka, R. and Williams, C. J. (2006). Role of the progressive ankylosis gene in cartilage mineralization. *Curr. Opin. Rheumatol.* **18**, 181-186.